A Design Method of Hybrid Analog/Asymmetrical-FIR Pulse-Shaping Filters with an Eye-Opening Control Option against Receiver Timing Jitter

Chia-Yu Yao

This paper presents a method of designing hybrid analog/asymmetrical square-root (SR) FIR filters. In addition to the conventional frequency domain constraints, the proposed method considers time-domain constraints as well, including the inter-symbol interference (ISI) and the opening of the eye pattern at the receiver output. This paper also reviews a systematic way to find the discrete-time equivalence of analog parts in a band-limited digital communication system. Thus, a phase equalizer can be easily realized to compensate for the nonlinear phase responses of the analog components. With the hybrid analog/SR FIR filter co-design, examples show that using the proposed method can result in a more robust ISI performance in the presence of the receiver clock jitter.

Keywords: Square-root filter, Nyquist filter, inter-symbol interference, eye pattern, linear programming, phase equalizer.

I. Introduction

A matched pair of square-root (SR) filters of a Nyquist filter used in the transmitter and the receiver of a band-limited digital communication system can provide zero inter-symbol interference (ISI) [1]. In practice, the SR filters are realized in FIR form. Conventionally, the SR filters are designed by directly designing the Nyquist filter with a non-negative frequency response (ignoring the linear-phase factor) [2]-[6], and then getting the matched SR transmitter and receiver filters by performing a spectral factorization on the Nyquist filter polynomial.

Although zero ISI is theoretically desired, in practice, it is not always necessary. In [7], [8], recognition of the "tolerable ISI" was proposed. The tolerable ISI should depend on the operating point, that is, the bit error rate (BER) vs. signal-to-noise ratio (SNR), of a band-limited digital communication system. As long as the ISI is smaller than the tolerable ISI, the BER performance of a communication system will not degrade significantly at the operating point. A small but non-zero ISI provides an increased degree of freedom in designing the SR filters.

Since there is interference and noise in the channel, the recovered receiver clock signal must suffer from some timing jitter [9] in practical implementations of band-limited communication systems. Thus, the synchronization between the transmitter and the receiver cannot be perfect. This receiver timing jitter will deteriorate the BER performance if the opening of the eye pattern is not sufficiently large. In [10]-[12], three different methods to design asymmetrical FIR SR filters with wide eye opening were proposed. With comparable eye
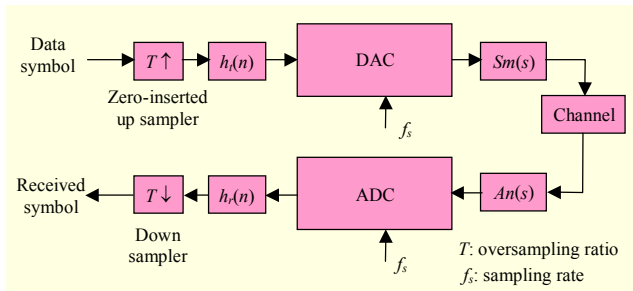
Fig. 1. Block diagram of band-limited digital communication system employing matched pulse-shaping filters to reduce ISI.

opening and stopband attenuation specifications, the length of the Nyquist filter of [10] is longer than that of [11] because the method in [10] employs the equiripple constraint in both the passband and the stopband, whereas the method in [11] only constrains the stopband gain. The method in [12] constrains the tail samples of the Nyquist filter's impulse response as well as the peak ripple error in the frequency domain. This results in a tradeoff between them. The example given in [12] shows that the filter, designed by the method in [12], which has good eye opening has difficulty in achieving low stopband gain.

On the other hand, there are analog filters and a digital-to-analog converter (DAC) in the system. Figure 1 shows a typical digital communication system in which $Sm(s)$ and $An(s)$ represent the smoothing filter and the anti-aliasing filter, respectively. These analog components will definitely affect the system performance. However, the design methods mentioned in [2]-[12] do not compensate for the nonlinear phase response. Thus, the overall system performance will be not as good as we might expect.

In [13], [14], design methods somewhat compensating for the analog parts were given. The method in [13] only considers the magnitude responses of the analog parts. However, the phase responses of analog filters are generally not linear. Thus, the method given in [13] is of limited application. Example 2 in section IV shows that only compensating for the magnitude response of analog parts is not sufficient to reduce the ISI in a band-limited communication system. In [14], it is assumed that the analog parts of the system are already phase-matched, but this does not show how to achieve phase-matching for analog filters. It is well known that an equalizer may approximately equalize the phase responses of analog filters. In this paper, we present a simple and systematic way to obtain such discrete-time phase equalizers. On the other hand, [13] and [14] do not take the eye opening of the system into account. Thus, the system employing filters designed by [13] or [14] may suffer from the receiver clock jitter.

In [15], a design strategy that considers both the analog portion and timing jitter was presented. In the transmitter, the cascade of the DAC, $Sm(s)$, and any block other than the SR filter $h_t[n]$ is called the nonFIR portion $u(t)$. In the receiver, the cascade of $An(s)$, the analog-to-digital converter (ADC), and any block other than the SR filter $h_r[n]$ is called the nonFIR portion $v(t)$. According to [15], the spectrum of the convolved signal DAC$\{h_t[n]\} * u(t)$ has to possess some desired shape. Since $u(t)$ includes a DAC, the sin(x)-over-x spectrum of the DAC in the passband has to be compensated for to a certain degree, either by $h_t[n]$ or an equalizer in the nonFIR portion. To ensure the match between the transmitter and the receiver, [15] employs $v(t)=u(-t)$ (and $h_t[n]=h_r[-n]$); that is, $v(t)$ also possesses the same spectrum of $u(t)$. Thus, another sin(x)-over-x spectrum in the passband has to be compensated for to a certain degree again in the receiver. However, there is only one DAC in the system, but the strategy of [15] needs to compensate for two sin(x)-over-x spectrum purposely. This implies that the strategy of [15] needs improvement.

In this paper, we employ a discrete-time equivalence to an analog channel that includes a DAC, a smoothing filter, an anti-aliasing filter, and an ADC. Then we insert the time-reversal of the discrete-time equivalence at the transmitter to compensate for the nonlinear phase distortion of analog parts. Since we know how to compensate the nonlinear phase response of the analog parts, we can focus on designing the Nyquist filter. Next, a composite method for designing an asymmetrical SR filter is proposed. The method takes the filter's stopband gain, the system's tolerable ISI, the system's eye opening, and the magnitude response of analog components into account simultaneously. Unlike [15], the proposed method does not require $v(t)=u(-t)$ and does not explicitly compensate for the sin(x)-over-x spectrum of the DAC. On the other hand, compensating for the effect of the DAC is implicitly considered in the problem formulation.

An adaptive equalizer in the receiver is so powerful against random channel distortions that no deterministic method can be used to compensate for them. In the case of pulse-shaping filters, the stopband attenuation, ISI, and eye opening are well-formulated. Therefore, by optimizing a performance index, the SR filter designed by the proposed method guarantees that the required system performance (for example, the ISI) is met, whereas an adaptive equalizer does not. On the other hand, when the channel contains some random distortions, the SR filters designed by the proposed method can work with an adaptive equalizer to improve the quality of the received signal.

This paper is organized as follows. In section II, we review a discrete-time channel model and the way of compensating for the nonlinear phase response of analog parts. In section III, the formulations of the proposed design method of asymmetrical SR filters are given. Numerical design examples are shown in section IV. Finally, conclusions are summarized in section V.

II. Review of a Discrete-Time Channel Model

Assume that the channel in Fig. 1 is a wideband linear-phase channel such that the channel model shown in Fig. 2 can be used for analysis. Let $a[m]$ denote the m-th transmitted data sample. The DAC is modeled as a zero-order hold block in Fig. 2 where T_0 represents the sampling period. The ADC is simply modeled as a sampler that takes samples at multiple instants $nT_0+\varepsilon$ where ns are non-negative integers and ε denotes the timing offset between the transmitter and the receiver. We assume that $0 \le \varepsilon < T_0$ for convenience. Let $h_{sm}(t)$ and $h_{an}(t)$ be the impulse responses of $Sm(s)$ and $An(s)$, respectively. Note that

$$h_{ana}(t) = h_{sm}(t) * h_{an}(t),$$

where $*$ is the continuous-time convolution operation. Since $h_{ana}(t)$ is causal, $r(t)$ can be derived as

$$r(t) = \sum_{m=0}^{\infty} a[m] \int_{\max(0,t-(m+1)T_0)}^{t-mT_0} h_{ana}(\tau) d\tau .$$

Note that $r[n] = r(nT_0 + \varepsilon)$, and let

$$\hat{h}_{t_1}^{t_2} = \int_{\max(0,t_1)}^{t_2} h_{ana}(\tau) d\tau, \quad \max(0,t_1) \le t_2, \qquad (1)$$

then

$$r[n] = \sum_{m=0}^{\infty} a[m] \hat{h}_{(n-m-1)T_0+\varepsilon}^{(n-m)T_0+\varepsilon}. \qquad (2)$$

Since $h_{ana}(\tau)$ is causal, $\hat{h}_{(n-m-1)T_0+\varepsilon}^{(n-m)T_0+\varepsilon} = 0$ when $(n-m)T_0+\varepsilon \le 0$, which implies that only those terms with $m \le n$ in (2) are non-zero. Therefore, (2) can be rewritten as

$$r[n] = \sum_{m=0}^{n-1} a[m] \hat{h}_{(n-m-1)T_0+\varepsilon}^{(n-m)T_0+\varepsilon} + a[n]\hat{h}_0^{\varepsilon}. \qquad (3)$$

Next, note that

$$h_{\Pi}^{\varepsilon}[n] = \begin{cases} \hat{h}_0^{\varepsilon}, & n = 0, \\ \hat{h}_{(n-1)T_0+\varepsilon}^{nT_0+\varepsilon}, & n = 1, 2, 3, ... \end{cases}$$

Thus, (3) can be rewritten as
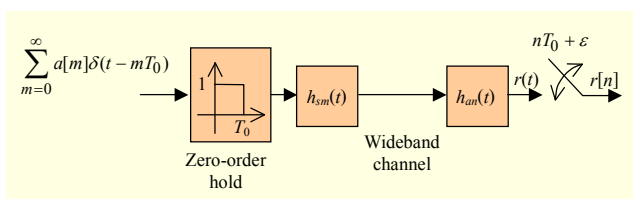
$$r[n] = a[n] * h_{\Pi}^{\varepsilon}[n],$$

Fig. 2. Baseband channel model.

where $*$ represents the discrete-time convolution operation. Unlike in [16], in which the discrete-time channel equivalence is from sampling the channel's impulse response directly, $h_{\Pi}^{\varepsilon}[n]$ is obtained from taking the effects of DAC and ADC into account and is computed by integrating the channel's impulse response segment by segment.

Hence, the channel in Fig. 2 can be modeled as a discrete-time convolution of the transmitted data samples $a[n]$, $n=0, 1, 2,...$, and the channel's equivalent discrete-time impulse response $h_{\Pi}^{\varepsilon}[n]$. Notably, $h_{ana}(t)$ is essentially time limited in practice [14], so is $h_{\Pi}^{\varepsilon}[n]$. Therefore, the channel can be modeled as an FIR channel in practice.

In general, since the sampling rate $1/T_0$ and the analog filters $Sm(s)$ and $An(s)$ are known a priori, we can use them to construct an M-tap FIR channel equivalence $\tilde{h}_{\Pi}^{\varepsilon}[n]$, $n=0, 1, ..., M-1$, by truncating the first M samples of $h_{\Pi}^{\varepsilon}[n]$. Next, assume that $\varepsilon = 0$, and let

$$h_{ins}[n] = \tilde{h}_{\Pi}^0[M-1-n]. \qquad (4)$$

Thus, $\tilde{h}_{\Pi}^0[n] * h_{ins}[n]$ possesses a linear phase response. In fact, the phase response of $h_{\Pi}^{\varepsilon}[n] * h_{ins}[n]$ is approximately linear. This implies that the nonlinear phase distortion introduced by $Sm(s)$ and $An(s)$ can be approximately compensated for by inserting $h_{ins}[n]$ in the transmitter or receiver.

It is noted that the values of $h_{\Pi}^{\varepsilon}[n]$ depend on ε. Therefore, a different timing offset ε leads to a different $h_{\Pi}^{\varepsilon}[n]$. The phase equalization FIR filter $h_{ins}[n]$ does not correct the sampling timing offset, it just approximately equalizes the phase response of the system. In order to obtain an optimum sampling timing, a clock recovery subsystem is required, which is beyond the scope of this paper.

III. Design of SR Filters with Robust Eye Openings

1. Formulations

By insertion of $h_{ins}[n]$, the phase response of the analog parts is approximately linearized. Next, note that

$$h_D[n] = \tilde{h}_{\Pi}^0[n] * h_{ins}[n].$$

The length of $h_D[n]$ is $2M-1$. For convenience, we assume that $h_D[n]$ spans across $n = -M+1, ..., -1, 0, 1, ..., M-1$.

Let N denote the length of the SR filters $h_t[n]$ and $h_r[n]$. It is known that $h_r[n]=h_t[N-1-n]$. The length of the Nyquist filter $h[n]$ $(=h_t[n] * h_r[n])$ becomes $2N-1$. For convenience, let us assume that $h[n]$ spans across $n = -N+1, ..., -1, 0, 1, ..., N-1$. Since $h[n]$ and $h_D[n]$ are symmetrical, the overall impulse
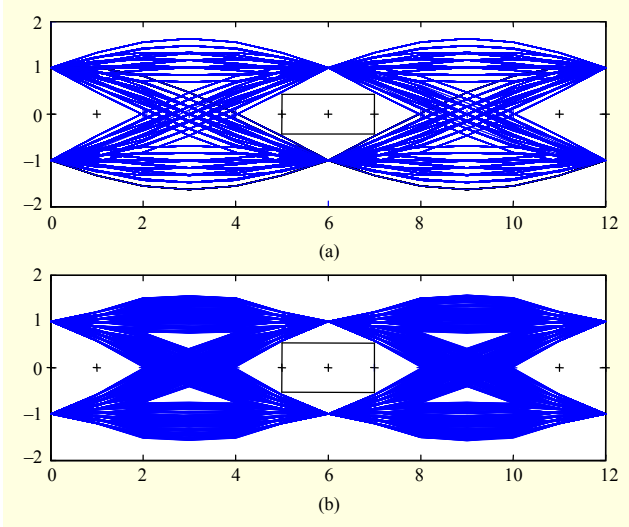
Fig. 3. Two eye patterns with $T=6$ result from two different Nyquist filters possessing same ISI.

response $h_c[n]=h[n]*h_D[n]$ is also symmetrical and can be represented as

$$h_c[n] = \sum_{m=1}^{N-1} h[m](h_D[n-m]+h_D[n+m]) + h[0]h_D[n], \quad (5)$$

where $|n| \leq N+M-2$. Let $\hat{N}=N+M-1$. The formula for calculating the system's ISI [17] becomes

$$\text{ISI} = \frac{\sum_{k=1}^{\left\lfloor \frac{\hat{N}-1}{T} \right\rfloor} |h_c[\pm kT]|}{h_c[0]}, \quad (6)$$

where T represents the number of samples per symbol (that is, T samples are sent for each symbol).

We can normalize the value of $h_c[0]$ as $1/T$ [5]. Since we adopt the tolerable ISI as a design parameter, if the tolerable ISI is denoted as γ_{ISI}, then (6) can be rewritten as

$$\sum_{k=1}^{\left\lfloor \frac{\hat{N}-1}{T} \right\rfloor} |h_c[kT]| \leq \frac{\gamma_{\text{ISI}}}{2T}. \quad (7)$$

Next, we develop a measurement for the eye-opening robustness of an eye pattern. Consider the two normalized eye patterns shown in Fig. 3 where the over-sampling ratio T is six. Hence, the time indices 0, 6, and 12 correspond to perfectly synchronous sampling instants. It is noted that the discrete-time samples are connected by straight lines in Fig. 3. These two eye patterns result from two different Nyquist filters that possess the same ISI at a multiple of T. The eye shown in Fig. 3(b) opens wider than that shown in Fig. 3(a).

Since system performance in the presence of receiver timing jitter is of great interest, the time indices one step away from the perfectly synchronous sampling instants are used to measure the eye-opening robustness (Fig. 3). The measure of

eye-opening robustness is similarly defined as ISI in [17] and has the form of

$$\frac{1}{\text{EYE}} = \frac{\sum_{k=1}^{\left\lfloor \frac{\hat{N}}{T} \right\rfloor} |h_c[kT-1]| + \sum_{k=1}^{\left\lceil \frac{\hat{N}-1}{T} \right\rceil - 1} |h_c[kT+1]|}{h_c[1]}. \quad (8)$$

A larger EYE value corresponds to a better eye opening. Note that if $T=2$, both the numerator and the denominator of (8) contain the term $h_c[1]$. In this case, even the maximum value of EYE is still poor. Therefore, the eye-opening technique presented in this paper applies only for cases where $T > 2$. Also note that the upper index of the second summation in the numerator of (8) is $\left\lceil (\hat{N}-1)/T \right\rceil - 1$. So, the summation will not contain the term $h_c[\hat{N}]$ if $\hat{N}-1$ is divisible by T.

In a manner similar to the ISI case, we denote γ_{EYE} as the specification of the eye opening. Then,

$$\sum_{k=1}^{\left\lfloor \frac{\hat{N}}{T} \right\rfloor} |h_c[kT-1]| + \sum_{k=1}^{\left\lceil \frac{\hat{N}-1}{T} \right\rceil - 1} |h_c[kT+1]| - \frac{h_c[1]}{\gamma_{\text{EYE}}} \leq 0. \quad (9)$$

Next, let us consider the frequency domain specifications. The zero-phase frequency response of the Nyquist filter is

$$H(\omega) = h[0] + \sum_{n=1}^{N-1} 2h[n]\cos n\omega. \quad (10)$$

A Nyquist filter stopband edge ω_s is specified by the roll-off factor α and the over-sampling ratio T as

$$\omega_s = \frac{(1+\alpha)\pi}{T}.$$

In the stopband, the magnitude response of a Nyquist filter is confined within the range $(0, \delta)$, where δ represents the stopband gain constraint. Therefore,

$$-h[0] - \sum_{n=1}^{N-1} 2h[n]\cos n\omega \leq 0, \ \omega \in [\omega_s, \pi], \quad (11)$$

and

$$h[0] + \sum_{n=1}^{N-1} 2h[n]\cos n\omega - \delta \leq 0, \ \omega \in [\omega_s, \pi]. \quad (12)$$

We note that there is no need to constrain a Nyquist filter's passband.

Finally, the frequency response at $\omega = \pi/T$ has to be examined. At that frequency, the magnitude response of $h_c[n]$ should be 1/2 [18], that is,

$$\sum_{n=1}^{\hat{N}-1} 2h_c[n]\cos \frac{n\pi}{T} = \frac{1}{2} - \frac{1}{T}. \quad (13)$$

Combining (7), (9), (11), (12), and (13), we formulate the primitive design problem as follows:

$$\text{minimize } \delta \qquad (14)$$

subject to

$$\sum_{k=1}^{\left\lfloor \frac{\hat{N}-1}{T} \right\rfloor} \left| h_c[kT] \right| \le \frac{\gamma_{\text{ISI}}}{2T},$$

$$\sum_{k=1}^{\left\lfloor \frac{\hat{N}}{T} \right\rfloor} \left| h_c[kT-1] \right| + \sum_{k=1}^{\left\lceil \frac{\hat{N}-1}{T} \right\rceil - 1} \left| h_c[kT+1] \right| - \frac{h_c[1]}{\gamma_{\text{EYE}}} \le 0,$$

$$-h[0] - \sum_{n=1}^{N-1} 2h[n]\cos n\omega \le 0, \quad \omega \in [\omega_s, \pi],$$

$$h[0] + \sum_{n=1}^{N-1} 2h[n]\cos n\omega - \delta \le 0, \quad \omega \in [\omega_s, \pi],$$

$$\sum_{n=1}^{\hat{N}-1} 2h_c[n]\cos\frac{n\pi}{T} = \frac{1}{2} - \frac{1}{T}.$$

The above formulation is not linear because the first and second constraints involve the absolute values of the linear combinations of the unknowns $h[0]$, $h[1]$,…, $h[N-1]$. However, it can be reformulated into a linear programming problem by using the following technique. For the first constraint, we introduce $\left\lfloor (\hat{N}-1)/T \right\rfloor$ non-negative slack variables $(a_k, k = 1, 2,…,\left\lfloor (\hat{N}-1)/T \right\rfloor)$ to relax the absolute values; that is, the first constraint is replaced by the following $2\left\lfloor (\hat{N}-1)/T \right\rfloor + 1$ constraints:

$$\sum_{k=1}^{\left\lfloor \frac{\hat{N}-1}{T} \right\rfloor} a_k \le \frac{\gamma_{\text{ISI}}}{2T}, \qquad (15)$$

and for $k = 1, 2,…,$ $\left\lfloor (\hat{N}-1)/T \right\rfloor$,

$$\pm\left(\sum_{m=1}^{N-1} h[m](h_D[kT-m] + h_D[kT+m]) + h[0]h_D[kT] \right) \le a_k.$$

$$(16)$$

For the second constraint, we introduce $\left\lfloor \hat{N}/T \right\rfloor +$ $\left\lceil (\hat{N}-1)/T \right\rceil - 1$ non-negative slack variables (b_k, $k = 1, 2,…,$ $\left\lfloor \hat{N}/T \right\rfloor$, and c_k, $k = 1, 2,…,$ $\left\lceil (\hat{N}-1)/T \right\rceil - 1$) to relax the absolute values. The new formulation for the second constraint becomes

$$\sum_{k=1}^{\left\lfloor \frac{\hat{N}}{T} \right\rfloor} b_k + \sum_{k=1}^{\left\lceil \frac{\hat{N}-1}{T} \right\rceil - 1} c_k - \frac{h_c[1]}{\gamma_{\text{EYE}}} \le 0, \qquad (17)$$

where

$$h_c[1] = \sum_{m=1}^{N-1} h[m](h_D[1-m] + h_D[1+m]) + h[0]h_D[1],$$

for $k = 1, 2,…,$ $\left\lfloor \hat{N}/T \right\rfloor$,

$$\pm\left(\sum_{m=1}^{N-1} h[m](h_D[kT-1-m] + h_D[kT-1+m]) + h[0]h_D[kT-1] \right)$$
$$\le b_k, \qquad (18)$$

and for $k = 1, 2,…,$ $\left\lceil (\hat{N}-1)/T \right\rceil - 1$,

$$\pm\left(\sum_{m=1}^{N-1} h[m](h_D[kT+1-m] + h_D[kT+1+m]) + h[0]h_D[kT+1] \right)$$
$$\le c_k. \qquad (19)$$

The unknowns are δ, $h[0]$, $h[1]$,…, $h[N-1]$, a_k, $k=1, 2,…,$ $\left\lfloor (\hat{N}-1)/T \right\rfloor$, b_k, $k=1, 2,…,$ $\left\lfloor \hat{N}/T \right\rfloor$, and c_k, $k=1, 2,…,$ $\left\lceil (\hat{N}-1)/T \right\rceil - 1$.

On the other hand, (14) is a semi-infinite programming problem because the third and the fourth constraints must be satisfied for all values of ω. This can be solved by employing the method shown in [5] that incrementally includes extreme points in the stopband of the current iteration to the constraints for the next iteration. This can be done by searching the stopband peak locations of the magnitude response of the coefficients obtained in the current iteration automatically. Hence, it is not necessary to sample ω in a very dense manner. According to the experience of testing many examples, using the iteratively incremental constraints at the extremal frequencies in the stopband is about 10 times faster than using extremely dense samples in the stopband of the original infinite number of constraints.

After changing the first and second constraints of (14) into (15) through (19) and employing the iteratively incremental constraints for the third and the fourth constraints of (14), one can iteratively use any standard linear programming problem solver to obtain the Nyquist filter coefficients. Next, the matched SR transmitter and receiver filters, $h_t[n]$ and $h_r[n]$, are determined by performing a spectral factorization on the Nyquist filter polynomial. Regarding the numerical accuracy issues mentioned in [5], we refer the reader to the more recent treatment of spectral factorization given in [19].

2. Estimating the Filter Length of the SR Filter

It is well known that there exists a simple formula for estimating the length of an optimal symmetric FIR filter. For example, [20] gives

$$N_1 = \frac{-20\log_{10}\sqrt{\delta_1\delta_2} - 13}{14.6\Delta f} + 1,$$

where N_1 is the estimated filter length, δ_1 and δ_2 correspond to the passband ripple magnitude and the stopband gain,

respectively, and Δf represents the width of the transition band.

Since the passband ripple is not constrained for a Nyquist filter $h[n]$, the stopband gain specification δ_s of the Nyquist filter is employed to the above formula twice, which leads to

$$N_1 = \frac{-20\log_{10}\delta_s - 13}{14.6\Delta f} + 1, \tag{20}$$

where the transition band Δf is equal to α/T for the Nyquist filter. Herein, N_1 corresponds to the degree of freedom of the Nyquist filter. There are two cases here. First, since three coefficients are strictly constrained, for every T sample of the Nyquist filter coefficients, if both ISI and EYE are constrained, the filter length of the Nyquist filter should be extended as

$$N_2 = \frac{T}{T-3}N_1.$$

Second, if only the ISI is constrained, then only one coefficient is constrained for every T sample of the Nyquist filter coefficients. Thus,

$$N_2 = \frac{T}{T-1}N_1.$$

Since $h[n] = h_t[n] * h_r[n]$, and $h_r[n]$ is matched to $h_t[n]$, N_2 has to be an odd number. Thus, the estimated filter length of the SR filter becomes

$$N = \left\lceil \frac{N_2 + 1}{2} \right\rceil. \tag{21}$$

The above equation provides the initial guess of the SR filter length in the following design procedure.

3. Design Procedure

Given the transfer functions of the two analog filters $Sm(s)$ and $An(s)$, roll-off factor α, over-sampling ratio T, tolerable ISI γ_{ISI}, eye-opening specification γ_{EYE}, and specification of stopband gain constraint δ_s of the Nyquist filter and having the design formulations (14) to (19), we developed the following design procedure:

i) Find the discrete-time equivalence, $h_\Pi^0[n]$, of the analog parts using the technique given in section II.

ii) Evaluate the M-tap phase-equalizing FIR filter $h_{ins}[n]$.

iii) Estimate the filter length N of the SR filter by (21).

iv) Use formulations (14) to (19) to obtain the Nyquist filter coefficients $h[n]$. In this step, several iterations may be required when the technique described in [5] is employed to avoid sampling ω in a very dense manner for the infinite number of constraints of (14).

v) If $\delta > \delta_s$, then $N = N+1$. Go to iv).

vi) Otherwise, perform a spectral factorization on $h[n]$ to obtain the SR filter coefficients $h_t[n]$ and $h_r[n]$.

Notably, in order to meet the system performance requirement, the proposed method requires a pair of SR filters and a separate phase equalizer in the system. At first, it seems that the system complexity is high. Fortunately, the length of the phase equalizer may not be long because, compared with the sampling rate, the transition bandwidth of the analog parts is usually not narrow in practice. For example, the 18-tap phase equalizer in example 1 of the next section can compensate for the nonlinear phase response of two cascaded third-order analog Butterworth filters. In this deep-submicron VLSI era, a filter with nominal length will not be troublesome.

IV. Design Examples

Example 1. Assume that both the smoothing filter at the transmitter and the anti-aliasing filter at the receiver are third-order lowpass Butterworth filters with the −3 dB frequency at 15 MHz. The sampling rate is set to be 70 Msamples/s. Hence,

$$Sm(s) = An(s)$$
$$= \frac{8.3717\times10^{23}}{s^3 + 1.8550\times10^8 s^2 + 1.7765\times10^{16} + 8.3717\times10^{23}},$$

and $T_0 = 1/(70\times10^6)\,\text{s}$. These two analog filters and the sampling rate are employed in all examples in this section for convenience.

The normalized frequency response of cascading the DAC and the analog filters can be expressed as

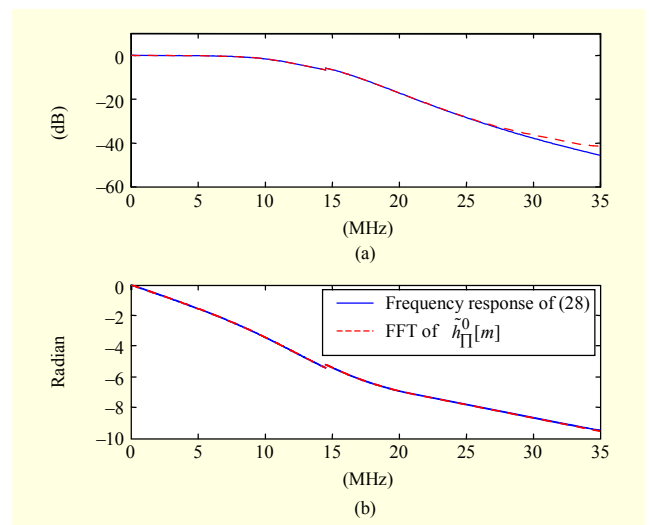$$H(f) = \frac{e^{-j\pi fT_0}\sin(\pi fT_0)}{\pi fT_0}Sm(j2\pi f)An(j2\pi f). \tag{22}$$

Fig. 4. (a) Magnitude responses and (b) phase responses of $H(f)$ and FFT of $\tilde{h}_\Pi^0[m]$.

By using the technique presented in section II, we obtain an 18-tap FIR filter $\tilde{h}_\Pi^0[m]$ of the discrete-time equivalence of the channel.

The frequency response of $H(f)$ and the FFT of $\tilde{h}_\Pi^0[m]$ are shown in Fig. 4. Figure 4(a) shows the magnitude responses, and Fig. 4(b) shows the phase responses. An effort has been made to keep the phase responses continuous across the π-borders. The two frequency responses match well at low frequencies. At frequencies near half of the sampling rate, the two frequency responses disagree with each other because $H(f)$ does not have the effect of aliasing caused by the sampler, whereas the FFT of $\tilde{h}_\Pi^0[m]$ does. Nevertheless, this example demonstrates that we can employ the technique presented in section II to model a digital communication channel shown in Fig. 2. Furthermore, to equalize the phase response of the analog parts in this example, we can employ the FIR filter $h_{\text{ins}}[m] = \tilde{h}_\Pi^0[17-m]$ at the receiver. The impulse response of $h_{\text{ins}}[m]$ is shown in Table 1.

Example 2. The design of a hybrid analog/asymmetrical-FIR pulse-shaping filter is verified in this example. The smoothing filter $Sm(s)$, anti-aliasing filter $An(s)$, and sampling rate are the same as those given in example 1. The over sampling ratio T equals 4, and the roll-off α equals 0.5. The three design goals are –40 dB stopband gain of the corresponding Nyquist filter, –30 dB tolerable ISI, and a 7 dB eye-opening specification of the system.

Three SR filters, $h_{t1}[m]$, $h_{t2}[m]$, and $h_{t3}[m]$ have been designed. The coefficients of them are shown in Table 2. Each SR filter corresponds to one of the following scenarios.

First, we ignore the effects of analog parts in the system and obtain an 18-tap $h_{t1}[m]$ by the method shown in [11]. The corresponding Nyquist filter $h_{t1}[m] * h_{t1}[17-m]$ satisfies the three design goals.

Second, we only consider the magnitude responses of the

Table 1. Coefficients of FIR filter $h_{\text{ins}}[m]$ used to equalize phase of analog parts in example 1.

$h_{\text{ins}}[0] = 1.6204 \times 10^{-5}$	$h_{\text{ins}}[9] = -4.2107 \times 10^{-2}$
$h_{\text{ins}}[1] = 4.7711 \times 10^{-4}$	$h_{\text{ins}}[10] = -7.6682 \times 10^{-2}$
$h_{\text{ins}}[2] = 6.4949 \times 10^{-4}$	$h_{\text{ins}}[11] = 1.0406 \times 10^{-2}$
$h_{\text{ins}}[3] = -6.3219 \times 10^{-4}$	$h_{\text{ins}}[12] = 2.4164 \times 10^{-1}$
$h_{\text{ins}}[4] = -3.0688 \times 10^{-3}$	$h_{\text{ins}}[13] = 4.1988 \times 10^{-1}$
$h_{\text{ins}}[5] = -2.4456 \times 10^{-3}$	$h_{\text{ins}}[14] = 3.2570 \times 10^{-1}$
$h_{\text{ins}}[6] = 6.2687 \times 10^{-3}$	$h_{\text{ins}}[15] = 9.3758 \times 10^{-2}$
$h_{\text{ins}}[7] = 1.6947 \times 10^{-2}$	$h_{\text{ins}}[16] = 3.6915 \times 10^{-3}$
$h_{\text{ins}}[8] = 5.6652 \times 10^{-3}$	$h_{\text{ins}}[17] = 0$

Table 2. Coefficients of three SR filters in example 2.

$h_{t1}[m]$:

$h_{t1}[0] = -6.0942671 \times 10^{-2}$	$h_{t1}[9] = -3.3755204 \times 10^{-2}$
$h_{t1}[1] = 3.6849007 \times 10^{-3}$	$h_{t1}[10] = -2.1573057 \times 10^{-2}$
$h_{t1}[2] = 8.5155633 \times 10^{-2}$	$h_{t1}[11] = 2.1852732 \times 10^{-2}$
$h_{t1}[3] = 1.9824302 \times 10^{-1}$	$h_{t1}[12] = 1.3742433 \times 10^{-2}$
$h_{t1}[4] = 2.8190563 \times 10^{-1}$	$h_{t1}[13] = 1.5470536 \times 10^{-2}$
$h_{t1}[5] = 2.6210301 \times 10^{-1}$	$h_{t1}[14] = -1.9685071 \times 10^{-2}$
$h_{t1}[6] = 2.0656040 \times 10^{-1}$	$h_{t1}[15] = -2.7340835 \times 10^{-2}$
$h_{t1}[7] = 6.6148636 \times 10^{-2}$	$h_{t1}[16] = 1.6922715 \times 10^{-3}$
$h_{t1}[8] = -8.1024145 \times 10^{-3}$	$h_{t1}[17] = 2.8230039 \times 10^{-2}$

$h_{t2}[m]$:

$h_{t2}[0] = -9.8005560 \times 10^{-2}$	$h_{t2}[13] = 2.6221385 \times 10^{-2}$
$h_{t2}[1] = -8.8899287 \times 10^{-2}$	$h_{t2}[14] = -1.6045033 \times 10^{-3}$
$h_{t2}[2] = -4.0463919 \times 10^{-2}$	$h_{t2}[15] = -1.4218584 \times 10^{-2}$
$h_{t2}[3] = 7.2252027 \times 10^{-2}$	$h_{t2}[16] = -5.0258694 \times 10^{-3}$
$h_{t2}[4] = 2.0117760 \times 10^{-1}$	$h_{t2}[17] = 1.1521196 \times 10^{-2}$
$h_{t2}[5] = 2.7895591 \times 10^{-1}$	$h_{t2}[18] = 1.7131378 \times 10^{-2}$
$h_{t2}[6] = 2.6626759 \times 10^{-1}$	$h_{t2}[19] = 8.0760093 \times 10^{-3}$
$h_{t2}[7] = 1.8044620 \times 10^{-1}$	$h_{t2}[20] = -4.4609185 \times 10^{-3}$
$h_{t2}[8] = 8.0551368 \times 10^{-2}$	$h_{t2}[21] = -8.0078147 \times 10^{-3}$
$h_{t2}[9] = 2.1907473 \times 10^{-2}$	$h_{t2}[22] = -1.0451159 \times 10^{-3}$
$h_{t2}[10] = 1.7263676 \times 10^{-2}$	$h_{t2}[23] = 1.0172637 \times 10^{-2}$
$h_{t2}[11] = 3.7667554 \times 10^{-2}$	$h_{t2}[24] = 2.2903524 \times 10^{-2}$
$h_{t2}[12] = 4.5057138 \times 10^{-2}$	$h_{t2}[25] = -2.3239211 \times 10^{-2}$

$h_{t3}[m]$:

$h_{t3}[0] = -8.9945397 \times 10^{-2}$	$h_{t3}[17] = 1.4279944 \times 10^{-2}$
$h_{t3}[1] = -6.9899120 \times 10^{-2}$	$h_{t3}[18] = 1.8189334 \times 10^{-2}$
$h_{t3}[2] = -8.8251586 \times 10^{-3}$	$h_{t3}[19] = 5.3197867 \times 10^{-3}$
$h_{t3}[3] = 1.1263071 \times 10^{-1}$	$h_{t3}[20] = -8.8206352 \times 10^{-3}$
$h_{t3}[4] = 2.3771957 \times 10^{-1}$	$h_{t3}[21] = -9.5825786 \times 10^{-3}$
$h_{t3}[5] = 2.9693128 \times 10^{-1}$	$h_{t3}[22] = 1.5337641 \times 10^{-3}$
$h_{t3}[6] = 2.5795204 \times 10^{-1}$	$h_{t3}[23] = 1.1546350 \times 10^{-2}$
$h_{t3}[7] = 1.5144053 \times 10^{-1}$	$h_{t3}[24] = 9.5630359 \times 10^{-3}$
$h_{t3}[8] = 4.5921595 \times 10^{-2}$	$h_{t3}[25] = -1.7867694 \times 10^{-3}$
$h_{t3}[9] = -3.8013075 \times 10^{-3}$	$h_{t3}[26] = -1.1236680 \times 10^{-2}$
$h_{t3}[10] = 5.1814748 \times 10^{-3}$	$h_{t3}[27] = -9.2093136 \times 10^{-3}$
$h_{t3}[11] = 3.3684475 \times 10^{-2}$	$h_{t3}[28] = 2.6236653 \times 10^{-3}$
$h_{t3}[12] = 4.0123666 \times 10^{-2}$	$h_{t3}[29] = 1.3525823 \times 10^{-2}$
$h_{t3}[13] = 1.6585917 \times 10^{-2}$	$h_{t3}[30] = 7.0846391 \times 10^{-3}$
$h_{t3}[14] = -1.3079162 \times 10^{-2}$	$h_{t3}[31] = -3.1852005 \times 10^{-2}$
$h_{t3}[15] = -2.1500346 \times 10^{-2}$	$h_{t3}[32] = 1.8795535 \times 10^{-2}$
$h_{t3}[16] = -5.8129289 \times 10^{-3}$	

analog parts in the system and obtain a 26-tap $h_{t2}[m]$ by the formulations given in [14]. The corresponding Nyquist filter $h_{t2}[m] * h_{t2}[25-m]$ satisfies the specification of –40 dB stopband gain. When a nonrealistic analog filter that possesses a zero-phase magnitude response equal to $|Sm(j2\pi f)An(j2\pi f)|$ is included in the channel, the –50 dB tolerable ISI and the 7 dB eye-opening specification are also satisfied.

Finally, we employ the phase equalizer $h_{ins}[m]$ given in Table 1 and use the procedure given in section III to obtain a 33-tap $h_{t3}[m]$. The corresponding Nyquist filter $h_{t3}[m] * h_{t3}[32-m]$ satisfies the specification of –40 dB stopband gain. When the analog filters $Sm(s)$ and $An(s)$ are included in the channel, and the phase equalizer $h_{ins}[m]$ is inserted after the ADC, the overall system satisfies the –30 dB tolerable ISI and the 7 dB eye-opening specifications.

Next, we consider the overall system with each SR filter. For $h_{t1}[m]$ and $h_{t2}[m]$, the system block diagram is the one given in Fig. 2. For $h_{t3}[m]$, in addition to the Fig. 2 block diagram, the phase equalizer $h_{ins}[m]$ is inserted after the ADC. Table 3 shows some performance indices of real systems employing $h_{t1}[m]$, $h_{t2}[m]$, and $h_{t3}[m]$. In Table 3, SBGAIN means the stopband gain of the Nyquist filter, and ISI and EYE are defined in (6) and (8), respectively. Although $h_{t1}[m]$ and $h_{t2}[m]$ can meet the design goals in their respective ideal scenarios, when $h_{t1}[m]$ and $h_{t2}[m]$ are put in a more realistic situation, the resulting ISI and EYE degrade from the ideal ones severely. On the other hand, the system employing $h_{t3}[m]$ and $h_{ins}[m]$ is the only one that satisfies all specifications.

Example 3. In this example, a receiver clock jitter is applied. The receiver clock may not be perfectly synchronous with the symbol timing at the transmitter. This will degrade the ISI performance. In this example, we compare the ISI performance of systems employing four SR filters under the receiver clock jitter. The first three SR filters are the same as those designed in example 2. The fourth SR filter is designed in a similar manner to $h_{t3}[m]$ except that no eye-opening specification is issued. Thus, the effectiveness of eye-opening control can be verified.

Using the procedure given in section III, we obtain an 11-tap $h_{t4}[m]$ whose coefficients are given in Table 4. The corresponding Nyquist filter $h_{t4}[m] * h_{t4}[10-m]$ reaches a –42.10 dB SBGAIN. The system employing $h_{t4}[m]$ has –30.10 dB ISI. However, since the eye-opening quality is not specified, it can only reach 4.70 dB EYE.

Figure 5 shows the ISI simulation results for four communication systems employing the four SR filters in the presence of the receiver clock jitter. The clock jitter is assumed to be white-Gaussian distributed. The x-axis is the standard deviation of the receiver clock jitter σ normalized by the sampling period T_0. Note that when the receiver clock jitter becomes worse, the ISI performance also becomes worse.

Table 3. Performance evaluation of systems employing $h_{t1}[m]$, $h_{t2}[m]$, and $h_{t3}[m]$ in example 2.

Performance index	System employs		
	$h_{t1}[m]$	$h_{t2}[m]$	$h_{t3}[m]$
SBGAIN (dB)	–40.05	–41.50	–40.20
ISI (dB)	–21.41	–23.43	–30.10
EYE (dB)	5.86	6.10	7.01

Table 4. Coefficients of SR filter without specifying eye-opening quality in example 3.

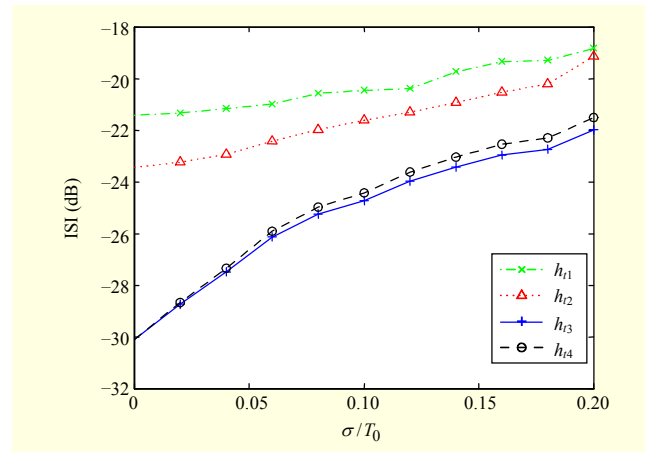| $h_{t4}[m]$:	
$h_{t4}[0] = 1.2347849 \times 10^{-1}$	$h_{t4}[6] = -3.5138469 \times 10^{-2}$
$h_{t4}[1] = 2.0805441 \times 10^{-1}$	$h_{t4}[7] = -7.6024637 \times 10^{-2}$
$h_{t4}[2] = 2.7791527 \times 10^{-1}$	$h_{t4}[8] = -5.9874178 \times 10^{-2}$
$h_{t4}[3] = 2.7321931 \times 10^{-1}$	$h_{t4}[9] = -2.3289513 \times 10^{-2}$
$h_{t4}[4] = 1.8909866 \times 10^{-1}$	$h_{t4}[10] = 4.1464322 \times 10^{-2}$
$h_{t4}[5] = 6.6350119 \times 10^{-2}$	

Fig. 5. ISI vs. σ / T_0 for four SR filters where σ is standard deviation of receiver clock jitter. For $h_{t3}[m]$ and $h_{t4}[m]$, a phase equalizer is used at receiver.

Since the designing of $h_{t1}[m]$ does not take the analog parts into account, and the designing of $h_{t2}[m]$ considers only the magnitude responses of the analog parts in the system, the ISI performances associated with $h_{t1}[m]$ and $h_{t2}[m]$ are much worse than those associated with the other two SR filters. For $h_{t3}[m]$ and $h_{t4}[m]$, the design considers the complete responses of the analog parts in the system, and the ISI performances associated with them at a low clock jitter are about the same. However, since the designing of $h_{t3}[m]$ takes the opening of the eye diagram into account, and the designing of $h_{t4}[m]$ does not, when the clock jitter becomes worse, the ISI performance associated with $h_{t3}[m]$ is about 0.6 dB lower than that
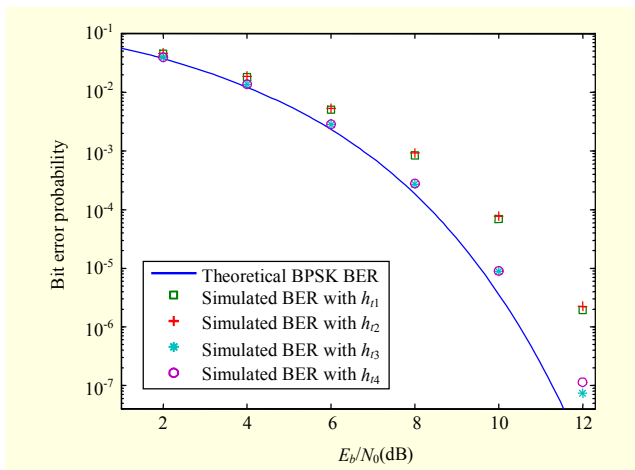
Fig. 6. BPSK BER simulations of four SR filters for $\sigma / T_0 = 0.2$. For $h_{t3}[m]$ and $h_{t4}[m]$, a phase equalizer is used at receiver.

Table 5. PARs of waveforms according to SR filters $h_{t1}[m]$, $h_{t2}[m]$, $h_{t3}[m]$, and $h_{t4}[m]$.

	$h_{t1}[m]$	$h_{t2}[m]$	$h_{t3}[m]$	$h_{t4}[m]$
PAR (dB)	3.32	5.11	4.97	3.24

associated with $h_{t4}[m]$. This verifies the effectiveness of controlling the opening of the eye.

Figure 6 shows the BPSK BER simulations of four SR filters for the case of $\sigma / T_0 = 0.2$. One can see that the cases that compensate for the effects of analog parts ($h_{t3}[m]$ and $h_{t4}[m]$) outperform the case that only compensates for the magnitude response ($h_{t2}[m]$) and the case that compensates for none of the effect of analog parts ($h_{t1}[m]$). The performances are about the same for the cases with $h_{t1}[m]$ and $h_{t2}[m]$ because the system performance of them for E_b/N_0 less than 12 dB is still noise-limited. Thus, compensating for only the magnitude response of analog parts is insufficient when the performance is limited by noise. On the other hand, the performance difference between the case with $h_{t3}[m]$ and the case with $h_{t4}[m]$ for SNR less than or equal to 10 dB is indistinguishable. However, when the SNR is 12 dB, the performance with $h_{t3}[m]$ is slightly better than the performance with $h_{t4}[m]$. The reason is the same as before. At low SNR, the system performance is limited by noise. When the SNR becomes sufficiently large, the ISI starts to affect the system performance. If the SNR is extremely large, the ISI will dominate the system performance. Hence, the eye-control mechanism takes effect only at a stringent scenario in which extremely low BER (or high SNR) is required.

Another important characteristic of the SR filter is its effect on the peak-to-average power ratio (PAR) of the transmitted waveform. The PAR can be evaluated by [21] as

$$ \text{PAR} = T \frac{\max_{0 \le i < T} \left(\sum_k \left| h_t (kT + i) \right| \right)^2}{\sum_k h_t^2(k)}. \qquad (23) $$

The PARs of the waveforms according to SR filters $h_{t1}[m]$, $h_{t2}[m]$, $h_{t3}[m]$, and $h_{t4}[m]$ are summarized in Table 5. We can

see that the PAR resulting from $h_{t4}[m]$ is the smallest one. Because we do not constrain the PAR in this paper, the PAR resulting from $h_{t3}[m]$ with eye control is 1.73 dB greater than that resulting from $h_{t4}[m]$ without eye control. On the other hand, if both the PAR and eye opening are constrained simultaneously, we will obtain an even longer SR filter than $h_{t3}[m]$. Thus, the hardware price we pay and the system performance we require should be carefully considered.

Although the ISI performance associated with $h_{t3}[m]$ is the best, the filter length of $h_{t3}[m]$ is three times the length of $h_{t4}[m]$. Therefore, if a stringent design is required, the designer can take the eye-control mechanism into account. Otherwise, ignoring the opening of the eye may lead to an imperfect but much less complicated SR filter.

V. Conclusion

A method for designing hybrid analog/asymmetrical-FIR SR filters with eye-control option has been presented. The proposed method takes the distortion of the analog components, SBGAIN of the filter, tolerable ISI of the system, and eye opening of the system into account.

By analyzing the continuous-time channel, this paper reviews the expression of an FIR equivalent channel model. In this expression, the nonlinear phase response of the analog parts can be easily linearized by an FIR equalizer that is constituted by time-reversing the FIR channel model. Once the nonlinear phase of the system can be compensated for, the formulations of designing the Nyquist filter are derived, and a linear-programming-based iterative design method is presented. After the Nyquist filter is obtained, the matched SR transmitter and receiver filters are determined by performing a spectral factorization on the Nyquist filter polynomial.

Design examples show that, without compensating for the nonlinear phase of the analog parts, the ISI of the system will be much worse than the desired value. On the contrary, when the nonlinear phase of the analog parts is compensated for by the method shown in section II, the ISI of the system can meet the design specification.

Design examples also show that the ISI will degrade in the presence of the receiver clock jitter. This paper demonstrates a method to control the opening of the eye such that the degradation of ISI can be reduced at a cost of increasing the SR

filter length and the waveform's PAR. In a stringent system, making the eye opening wider can improve the system performance at high SNR. On the other hand, if the required performance is not so critical, the eye-opening control can be ignored. Therefore, the system engineers should make a tradeoff between the ISI performance and the complexity of the SR filters.

References

[1] J.G. Proakis and M. Salehi, *Communication Systems Engineering,* 2nd ed., Upper Saddle River, NJ: Prentice Hall, 2002.

[2] A.C. Salazar and V.B. Lawrence, "Design and Implementation of Transmitter and Receiver Filters with Periodic Coefficient Nulls for Digital Systems," *IEEE Int. Conf. Acoust. Speech, Signal Process.*, vol. 7, May 1982, pp. 306-310.

[3] P.R. Chevillat and G. Ungerboeck, "Optimum FIR Transmitter and Receiver Filters for Data Transmission over Band-Limited Channels," *IEEE Trans. Commun.*, vol. COM-30, Aug. 1982, pp. 1909-1915.

[4] J.K. Liang, R.J.P. de Figueiredo, and F.C. Lu, "Design of Optimal Nyquist, Partial Response, *N*-th Band, and Nonuniform Tap Spacing FIR Digital Filters Using Linear Programming Techniques," *IEEE Trans. Circuits. Syst.*, vol. CAS-32, Apr. 1985, pp. 386-392.

[5] H. Samueli, "On the Design of Optimal Equiripple FIR Digital Filters for Data Transmission Applications," *IEEE Trans. Circuits. Syst.*, vol. 35, Dec. 1988, pp. 1542-1546.

[6] H. Samueli, "On the Design of FIR Digital Transmission Filters with Arbitrary Magnitude Specifications," *IEEE Trans. Circuits. Syst.*, vol. 38, Dec. 1991, pp. 1563-1567.

[7] C.-Y. Yao, "The Design of Square-Root-Raised-Cosine FIR Filters by an Iterative Technique," *IEICE Trans. Fundamentals*, vol. E90-A, Jan. 2007, pp. 241-248.

[8] C.-Y. Yao and A.N. Willson, Jr., "The Design of Symmetric Square-Root Pulse-Shaping Filters for Transmitters and Receivers," *Proc. IEEE Int. Symp. Circuits Syst.*, May 2007, pp. 2056-2059.

[9] W.C. Lindsey and M.K. Simon, *Telecommunication Systems. Engineering*, Englewood Cliffs, NJ: Prentice Hall, 1973.

[10] B. Farhang-Boroujeny and G. Mathew, "Nyquist Filters with Robust Performance Against Timing Jitter," *IEEE Trans. Signal Process.*, vol. 46, Dec. 1998, pp. 3427-3431.

[11] C.-Y. Yao and A.N. Willson, Jr., "The Design of Asymmetrical Square-Root Pulse-Shaping Filters with Wide Eye-Openings," *Proc. IEEE Int. Symp. Circuits Syst.*, May 2008, pp. 2665-2668.

[12] P. Boonyanant and S. Tantaratana, "Design and Hybrid Realization of FIR Nyquist Filters with Quantized Coefficients and Low Sensitivity to Timing Jitter," *IEEE Trans. Signal Process.*, vol. 53, Jan. 2005, pp. 208-221.

[13] J.O. Coleman and D.W. Lytle, "Linear-Programming Techniques for the Control of Intersymbol Interference with Hybrid FIR/Analog Pulse Shaping," *Proc. IEEE Int. Conf. Commun.*, Chicago, IL, June 1992, pp. 793-798.

[14] T.N. Davidson, Z.-Q. Luo, and K.M. Wong, "Design of Orthogonal Pulse Shapes for Communications via Semidefinite Programming," *IEEE Trans. Signal Process.*, vol. 48, May 2000, pp. 1433-1445.

[15] J.O. Coleman, "Linear-Programming Design of Data-Communication Pulses Tolerant of Timing Jitter or Multipath," *Proc. 5th Int. Conf. Wireless Commun.*, Calgary, Alta., Canada, July 1993, pp. 341-352.

[16] J. Liu, "Be Cautious When Using the FIR Channel Model with the OFDM-Based Communication Systems," *IEEE Trans. Veh. Technol.*, vol. 58, no. 3, 2008, pp. 1607-1612.

[17] C.-L. Chen and A.N. Willson, Jr., "A Trellis Search Algorithm for the Design of FIR Filters with Signed-Powers-of-Two Coefficients," *IEEE Trans. Circuits Syst. II*, vol. 46, no. 1, Jan. 1999, pp. 29-39.

[18] P. Siohan and F.M. de Saint-Martin, "New Designs of Linear-Phase Transmitter and Receiver Filters for Digital Transmission Systems," *IEEE Trans. Circuits. Syst. II*, vol. 46, no. 4, Apr. 1999, pp. 428-433.

[19] H.J. Orchard and A.N. Willson, Jr., "On the Computation of a Minimum Phase Spectral Factor," *IEEE Trans. Circuits. Syst. I*, vol. 50, Mar. 2003, pp. 365-375.

[20] J.G. Proakis and D.G. Manolakis, *Digital Signal Processing Principles, Algorithm, and Applications,* 3rd Ed., Upper Saddle River, NJ: Prentice Hall, 1996.

[21] B. Farhang-Boroujeny, "A Square-Root Nyquist (M) Filter Design for Digital Communication Systems," *IEEE Trans. Signal Process.*, vol. 56, May 2008, pp. 2127-2132.

Chia-Yu Yao received the BS from National Taiwan University in 1985, and his MS and PhD from UCLA in 1988 and 1992, respectively, all in electrical engineering. From 1985 to 1987, he served as a Second Lieutenant at Chinese Military Academy. From 1990 to 1991, he was with LinCom Corporation, Los Angeles, engaged in a program of satellite communication system analysis funded by the NASA. In 1992, he joined the Department of Electronic Engineering, Huafan University, Taipei, Taiwan, R.O.C. In 2006, he joined the Department of Electrical Engineering, National Taiwan University of Science and Technology, Taipei, Taiwan, R.O.C., where he is currently an associate professor. His research interests include digital filter design, CMOS RF integrated circuits, and neural networks. Dr. Yao was one of the recipients of the Group Achievement Award from Computer Sciences Corporation in 1991. In 2000, he was the adviser of the Best Student Paper Award in signal processing for the National Symposium on Telecommunications in Taiwan. He was the adviser of the Praise Award of Student Paper Contest held by the Chinese Institute of Electrical Engineering in 2009.